Photocross-linking of Low-Density Polyethylene. III. Supermolecular Structure Studied by SALS

BAO JUN QU[1] and BENGT RÅNBY[2,*]

[1]Structure Research Laboratory, University of Science and Technology of China, 230026 Hefei, Anhui, China;
[2]Department of Polymer Technology, The Royal Institute of Technology, S-100 44 Stockholm, Sweden

SYNOPSIS

The supermolecular structure of photocross-linked polyethylene (XLPE) has been studied by small-angle light scattering (SALS). The data show that the spherulitic structure of XLPE gradually deteriorates with increasing degree of cross-linking and increasing irradiation temperature from well-developed spherulites to rodlike aggregates and disordered lamellar structures. A photocross-linked sample of PE has lower crystallinity, smaller crystallites, and smaller spherulites than does the original sample. At high degrees of cross-linking, the SALS patterns show little or no spherulitic structure. Results with photocross-linked polyethylene demonstrate that the overall effect of cross-linking on the morphological structure is similar to that of an increase in molecular weight of the polymer. © 1993 John Wiley & Sons, Inc.

INTRODUCTION

Changes of thermodynamic properties such as density, melting point, and heat of fusion of photocross-linked polyethylene (XLPE) have been shown to be related to the degree of cross-linking and the irradiation temperature during cross-linking as described in Part II of this series.[1] These properties are correlated with the level of crystallinity, the morphological structure of the lamellar crystallites, and the associated interfacial and amorphous regions. The order of crystalline organization, the supermolecular structure, and the spherulitic morphology are widely investigated in crystalline polymers. The strong influence of photocross-linking on these properties makes it a matter of interest to further study the spherulitic structure and other morphological forms of XLPE.

It has been demonstrated that the morphological structure of semicrystalline polymers such as polyethylene is related to spherulite formation.[2-11] Small-angle light-scattering (SALS) patterns can be used to characterize the size and the degree of order of the spherulites and other morphologies formed in bulk, depending on the molecular weight and the crystallization temperature.[4,6,7] The SALS technique and theory has been developed by Stein et al.[2,3,12-15] It provides some distinct advantages over polarized light microscopy in studying the supermolecular structure. First, the subjectiveness of the interpretation of the morphological types is eliminated as well as artifacts related to the use of thin films. Second, the radii of spherulites are easily determined from the SALS patterns, which are sensitive to changes in size and shape of the spherulites. Third, a detailed morphological description, i.e., spherulites, rodlike aggregates, and randomly oriented lamellae, can be clearly obtained utilizing SALS patterns even if the scattering entities are mixed in a sample. In short, SALS is a powerful method for characterization of the supermolecular structure of a crystalline polymer.

Observations of PE spherulites by the SALS technique have been made by several authors,[2-11] but applications to cross-linking systems have as yet been limited. There is no paper to date about SALS studies of photocross-linked PE. In the present work, SALS is the major experimental technique used in studying photocross-linked PEs, since it has been shown to be an excellent method for the detection of different morphological forms or super-

* To whom correspondence should be addressed.

Journal of Applied Polymer Science, Vol. 49, 1799–1807 (1993)
 CCC 0021-8995/93/101799-09

molecular structures in polymer films.[16-21] The main purpose is to investigate changes of supermolecular structures in PE caused by photocross-linking and to interpret the corresponding changes of thermodynamic parameters derived in the previous paper.[1]

EXPERIMENTAL

Materials

Low-density polyethylene (LDPE) DFDS 6600 and linear LDPE 8016 (LLDPE) were obtained from Neste Polyeten AB, Sweden; LDPE Statoil L400, from Statoil A/S, Norway; and high-density polyethylene (HDPE) Lupolen 5261 Z (L), from BASF and Hostalen 412 (H) from Hoechst AG. An HDPE sample was used with the ratio of $L/H = 8/2$. All samples used in this work contained 1 wt % 4-chlorobenzophenone (4-CBP) as initiator and 1 wt % triallyl cyanurate (TAC) as cross-linker. The properties of the four kinds of PE before photocross-linking are listed in Table I.

Preparation of Film Samples

All the samples were prepared by the same method in order to reduce the effects of various factors of the photocross-linking processes on the morphological properties of XLPE. Fifty grams of PE power or granules were mixed with 1 wt % 4-CBP and 1 wt % TAC for 10 min at 160–200°C in a Brabender Plasticorder. The film samples were prepared in a hotpress device and UV-irradiated in a UV-CURE with N_2 atmosphere at a preset temperature of 140°C for LDPE and LLDPE and 150°C for HDPE,[1] using a 2 kW Philips HPM 15 lamp, at a 10 cm distance from the surface of the sample. After UV irradiation, the molten sample was rapidly cooled to room temperature in air. The basic procedures for preparing photocross-linked films by mixing, hotpressing, and UV irradiation and for cooling the polymer samples after photocross-linking were essentially the same as used previously.[1]

The thickness of sample for SALS was limited to 20–50 μm in order to avoid large amounts of secondary scattering, which obscures details of the primary scattering pattern.

Small-Angle Light Scattering

An He–Ne laser is used as source of polarized, monochromatic light ($\lambda_0 = 6328$ Å). The film sample is placed between the analyzer and the polarizer (Fig. 1). The plane of polarization of the analyzer is perpendicular to that of the polarized laser beam (the scattering photograph obtained is called an H_v pattern). The molded and photocross-linked films are held between microscope glass slides and immersed in silicone oil to minimize surface scattering. The H_v SALS patterns were recorded on Polaroid type 55 films. The exposure time and the sample-to-film distance are adjustable to give sufficient intensity. A diagram of the photographic light scattering apparatus is given in Figure 1.

Stein and co-workers[2,3] developed a theory for the SALS of spherulites. The theory predicts an H_v scattering pattern appearing as a four-leaf clover pattern (Fig. 2), observed with maxima at odd multiples of the 45° azimuthal angle (μ) and at an angle θ_{max} between the incident and scattered beams characteristic of the radius of the spherulite. The predicted and observed positions of the maxima for $\mu = 45°$ indicate an orientation of the crystal optical axes parallel or perpendicular to the spherulite radius. The size of the spherulite is calculated by eq. (1) in which θ_{max} is obtained from (i) the measured distance of the center of one of the lobes from the center of the pattern and (ii) the known sample-to-film distance (see Fig. 1).

The spherulite size is calculated from the H_v SALS pattern using the formula[2,5]

Table I The Properties of PE Samples before Photocross-linking[a]

Sample	Density (g cm^{-3})	T_m (°C)	Crystallinity (%)	Spherulite Radius (μm)
(a) DFDS 6600	0.924	110.0	53.2	8.0
(b) Statoil L400		112.0		8.9
(c) LLDPE8016		126.0		2.2
(d) HDPE	0.961	135.0	77.0	4.0

[a] The crystallinity is measured by wide-angle X-ray diffraction, and the radius of the spherulites, by SALS.

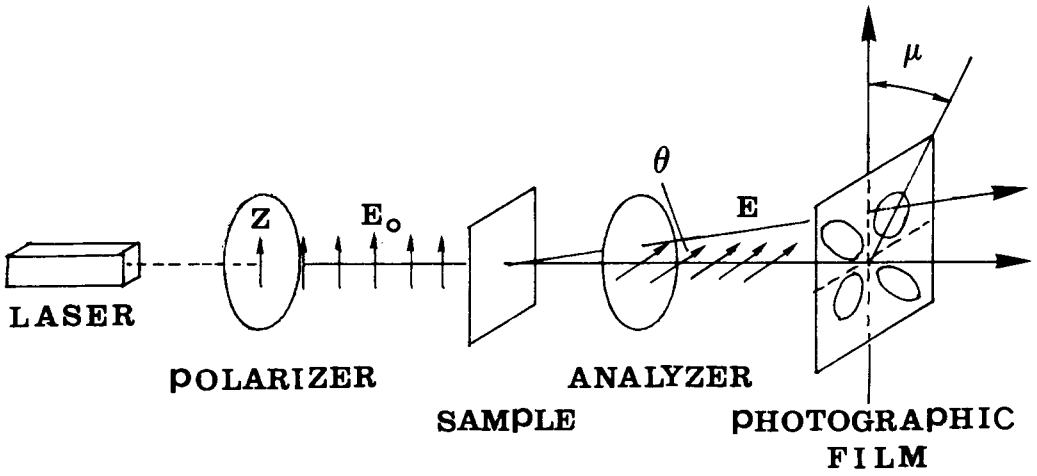

Figure 1 Schematic diagram of photographic light-scattering apparatus used in this experiment.

$$R = \frac{4.09\lambda_0}{4\pi n \sin\left(\frac{\theta_{max}}{2}\right)} \quad (1)$$

In the above equation, R, λ_0, θ, and n denote, respectively, spherulite radius, wavelength in vacuum, scattering angle, and refractive index in the PE film, taken as $n = 1.5$. Values of θ_{max} and spherulite radius (R) thus determined are summarized in Tables I–IV.

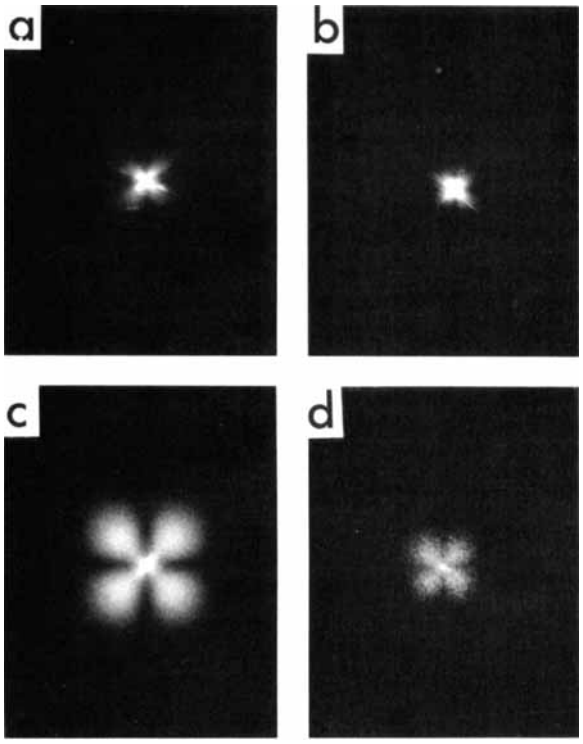

Figure 2 The experimental H_v patterns of four kinds of PEs before photocross-linking: (a) DFDS 6600; (b) Statoil L 400; (c) LLDPE 8016; (d) HDPE: $L/H = 8/2$.

Other Analysis of Samples

The degree of crystallinity was measured by wide-angle X-ray diffraction. The density was measured on an alcohol–water gradient column. The melting point was recorded by a Perkin-Elmer Model DSC-2 instrument. The gel content was obtained by extraction of the cross-linked samples in boiling *p*-xylene. The above methods were described in detail in the previous paper.[1]

RESULTS AND DISCUSSION

Light-Scattering Background

Before we present our experimental results and interpret the data in terms of supermolecular structure related to photocross-linking, we first summarize the background of scattering theory and structural models, which have been developed by Stein et al.[2–4] and Mandelkern et al.[6–8] PE crystallites are usually arranged in spherical aggregates, spherulites, with different radial and tangential refractive indices. This optical anisotropy is a consequence of the arrangement of the anisotropic crystallites inside the spherulites.

Many studies have shown[4,6–8,14–16] that spherulites are not formed in all crystalline polymers. SALS patterns are observed also for structures that are

Table II The SALS Data Correlated with Gel Content and Crystallinity in Figure 3

Sample	Irrad Temp (°C)	θ_{max} (Degree)	Radius (μm)	Gel (%)	Crystallinity (%)
DFDS 6600					
(a)		1.99	8.0		53.2
(b)	100	2.18	7.2	45.5	52.7
(c)	110			53.4	51.3
(d)	140			65.1	49.1
HDPE					
(e)		4.33	3.6		77.0
(f)	110	5.08	3.1	58.1	71.0
(g)	135	6.97	2.3	75.1	64.8
(h)	150	7.80	2.0	85.0	60.2

nonspherulitic. Other structures such as rodlike aggregates of lamellae can be developed, and in some cases, no organized forms of lamellar crystallites are found at all. In this study, we shall not present a complete survey of all the different theoretical models that have been proposed. Rather, we shall only select some models that provide an adequate interpretation of our results. It has been reported[4,6–8] that there are many types of morphological forms identified from SALS patterns for linear PE, depending on molecular weight and crystallization temperature. Among them, the three major types of supermolecular structures and the corresponding characteristics of the H_v SALS patterns are as follows:

1. Spherulitic structures. There are three different types of spherulitic patterns that can be distinguished from each other: (A) a fourleaf clover appearance of the H_v pattern with fourfold symmetry and four lobes of intensity interpreted as due to well-developed spherulitic structure; (B) a variant of the (A) pattern with a "shaped like a 'tennis racquet' appearance"; and (C) a further degeneration of the spherulitic pattern characteristic of a figure "X." Pattern C has a fourfold symmetry and a definite maximum in θ at $\mu = 45°$. SALS patterns of B and C type could be interpreted theoretically in terms of multiple scattering and imperfections in shape or imperfections of the internal order of the spherulites. Thus, the three different types of spherulitic patterns essentially represent different levels of order within the spherulite.

Table III The SALS Data Correlated with Gel Content and Crystallinity in Figure 4

Sample	Irradiation Conditions	θ_{max} (Degree)	Radius (μm)	Gel (%)	Crystallinity (%)
DFDS 6600 100°C					
(a)	10 s	2.45	6.5	34.9	53.0
(b)	20 s	2.73	5.7	48.6	52.2
(c)	40 s			63.5	49.5
(d)	80 s			72.9	45.6
(e)	160 s			79.2	44.5
DFDS 6600 140°C					
(f)	10 s	2.73	5.7	48.5	51.9
(g)	20 s			65.2	49.1
(h)	40 s			73.2	45.0
(i)	80 s			80.3	44.1
(j)	160 s			83.1	43.2

Table IV The SALS Data and Gel Content of LLDPE

Sample	Irradiation Conditions	θ_{max} (Degree)	Radius (μm)	Gel (%)
100°C				
(a)	5 s	7.2	2.2	0.6
(b)	10 s	7.2	2.2	5.0
(c)	20 s	7.2	2.2	23.1
(d)	40 s	7.3	2.1	32.3
(e)	80 s	7.7	2.0	56.0
140°C				
(f)	5 s	8.5	1.8	1.1
(g)	10 s	11.3	1.8	12.6
(h)	20 s	11.3	1.2	43.3
(i)	40 s	11.3	1.2	67.3
(j)	80 s	12.9	1.1	82.0

For convenience, we shall designate these spherulites as types A, B, and C, respectively, in the subsequent discussion.

2. Rodlike aggregates of lamellar structure that also have several modes. Among them, there are two scattering patterns: One gives a predominantly azimuthally independent appearance superimposed by a fourfold symmetry[8] and another gives an azimuth-dependent "+" appearance[7] with a fourfold symmetry but a much greater intensity at the center as seen in our experimental results. We classify these SALS patterns as types D and E, respectively. The equations for the H_v scattered intensity of these rodlike patterns are more complex than for spherulites.[16,17]
3. Randomly oriented or disordered lamellar structure. The H_v scattering pattern is circular symmetric and is designated as type F. The scattering intensity of the type F pattern is azimuthally independent and has its maximum at the center. An important result in the previous works[4,6-8] is that under rapid crystallization conditions the spherulite structure is strongly dependent on molecular weight and crystallization temperature. There is a molecular weight range from 1.54×10^4 to 8.5×10^5, where well-defined spherulitic structures are observed.[7]

The above models represent only a few among many discussed in the literature and they have been selected for the interpretation of the experimental results obtained in our work.

RESULTS

Spherulitic Structures before Photocross-linking

Our experimental results will be discussed and interpreted in terms of the light-scattering theory and the structural models described. Spherulitic structures are, in general, observed in crystalline PE. The changes in the supermolecular structure of PE caused by photocross-linking have been identified in the SALS patterns. Figure 2 shows the H_v patterns of four kinds of uncross-linked PE films after rapid crystallization from the melt. It is apparent that they have spherulitic structures of A, B, and C types, although the apparent differences are in the size and shape of the spherulites. The HDPE and LLDPE [Fig. 2(d) and (c)] have well-developed spherulitic structures of types A and B, respectively. The two LDPE samples [Fig. 2(a) and (b)] show spherulitic structure type C. The size of the spherulites are listed in Table I. Spherulitic radii are of the order 8–9 μm for LDPE and 2–4 μm for LLDPE and HDPE obtained from the SALS patterns of the uncross-linked PE films. These data are in good agreement with results reported by other authors.[5,22]

Effect of Irradiation Temperature on Morphology

The H_v SALS patterns for DFDS 6600 and HDPE samples photocross-linked by 15 s irradiation at different temperatures (below, at, and above the melting point T_m) are shown in Figure 3. The SALS patterns (b) and (f) for the samples cross-linked below T_m have a similar size and shape as those of uncrosslinked samples (a) and (e), respectively, with their spherulite radii given in Table II. For the samples cross-linked at T_m, patterns (c) and (g) become more diffuse than those in (b) and (f). Pattern (c) seems to have transitional supermolecular structure and gives a predominantly azimuthally independent appearance superimposed by a weak fourfold symmetry, classified as a rodlike spherulitic structure of D type. Pattern (g) still has the same spherulite structure although deteriorated. Upon cross-linking above T_m, more diffuse patterns are obtained that are characteristic of a greater degree of disorder with the supermolecular structure as seen in patterns (d) and (h). The (d) pattern with circular symmetry for the LDPE sample suggests that it has developed a randomly oriented lamellar structure classified as F type. Such a disordered pattern F has been described[2-4,6-8] on the basis of a spherulitic structure within which the optical axes are not perfectly aligned with respect to the radii but

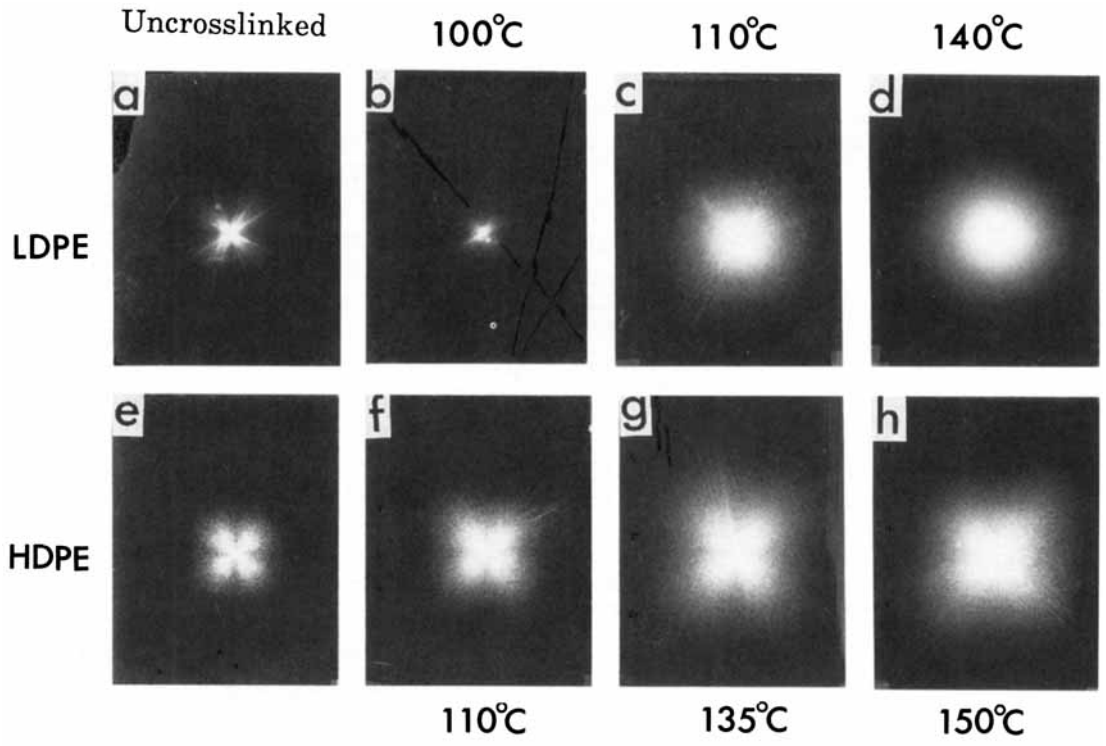

Figure 3 The effect of irradiation temperature on the H_v SALS patterns of DFDS 6600 and HDPE samples. Irradiation time: 15 s. LDPE: (a) before cross-linking; (b) 100°C; (c) 110°C; (d) 140°C. HDPE: (e) before cross-linking; (f) 110°C; (g) 135°C; (h) 150°C.

deviate from the ideal orientation in a random manner. On the other hand, pattern (h) for HDPE only becomes more diffuse, the light scattering becomes stronger at the center with a distinct fourfold symmetry, and the spherulite radius has become smaller, as seen in Table II. The corresponding changes of gel content and crystallinity are listed in Table II. As can be noted, increasing irradiation temperature and gel content cause a progressive deterioration of the initial spherulitic morphology characteristic of the uncross-linked samples. This gradual deterioration of the spherulitic structure occurs with a simultaneous decrease in the level of crystallinity.

Effect of Degree of Cross-linking on Morphology

The effects of the degree of cross-linking on the spherulitic structures of samples cross-linked below or above the melting point are further shown in Figure 4 for the DFDS 6600 sample. The H_v SALS patterns in Figure 4 show typical changes of supermolecular morphology, whose spherulitic structure and perfection progressively deteriorate as the degree of cross-linking increases. The upper-row H_v patterns in Figure 4 obtained for irradiation times of 10–160 s at 100°C (below T_m) show a gradual deterioration from spherulitic morphology characteristic of a fourfold "X" (designated as type C) to rodlike morphological form ("+" shaped, type E) with increasing irradiation time, i.e., to rodlike aggregates of lamellar structure according to the literature.[4,6,7] It can be seen that the H_v patterns (a) and (b) within the irradiation time of 20 s are similar to that of an uncross-linked DFDS 6600 sample having spherulitic structure of type C. This could mean that certain spherulitic morphological forms continue to exist in samples with a low degree of cross-linking. But patterns (d) and (e) at the irradiation times of 80 and 160 s show the azimuth-dependent "+" appearance and become more and more diffuse; these are characteristics of rodlike aggregates of lamellar structure classified as E type. Pattern (c) seems to be a transitional region given by a weak fourfold symmetry with great intensity at the center classified as a type D, rodlike lamellar structure. On the other hand, the bottom-row H_v patterns obtained from corresponding irradiation times of 10–160 s at 140°C (above T_m) show drastic changes in the morphological structure of XLPE with increasing irradiation time. After only 10 s irradiation, pattern (f) shows a nondistinct "X"-type appearance (a deteriorated spherulite type C). The

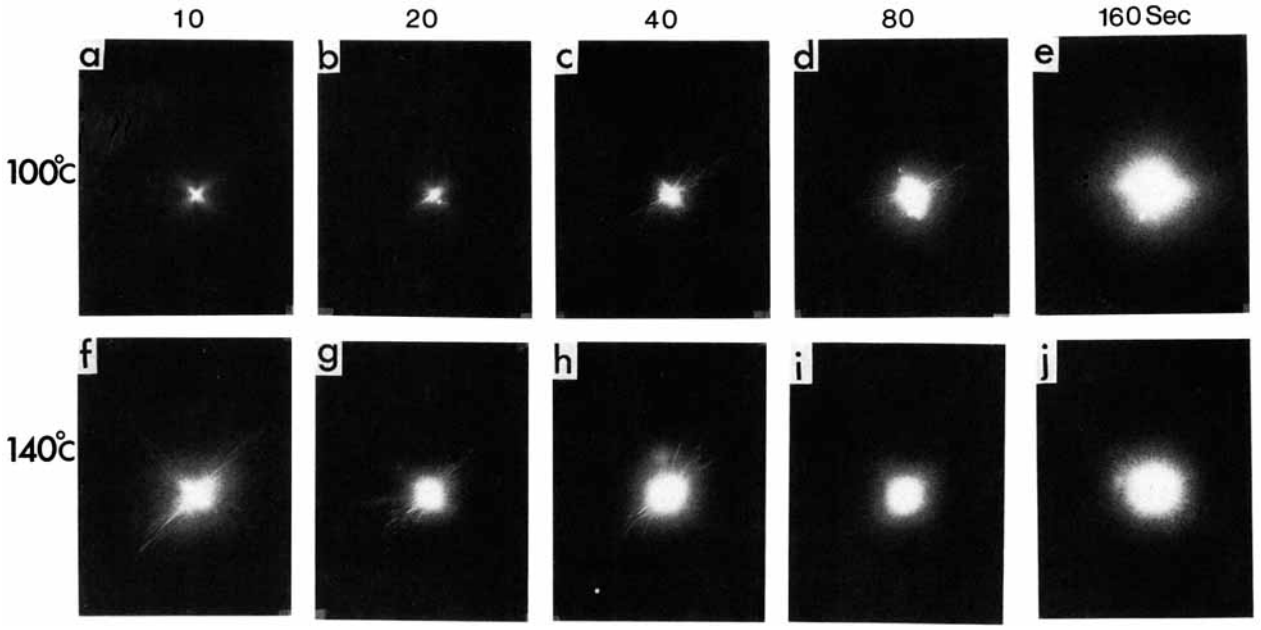

Figure 4 The effect of irradiation time on the supermolecular structures of DFDS 6600 samples. Upper row: cross-linked at 100°C (below T_m)—(a) 10 s; (b) 20 s; (c) 40 s; (d) 80 s; (e) 160 s. Bottom row: cross-linked at 140°C (above T_m)—(f) 10 s; (g) 20 s; (h) 40 s; (i) 80 s; (j) 160 s.

morphology in the cross-linked sample of 20 s irradiation has completely lost the spherulitic structure as seen in pattern (g) similar to that in Figure 4(c), an azimuth-dependent "+" appearance classified as D type. Patterns (h)–(j) have circularly symmetric appearances due to the disordered lamellar structure of the F type.[4,6,7] This can be attributed to the low level of crystallinity in the highly cross-linked samples (Table III).

Go et al.[4] suggested that a causal relation exists between the levels of crystallinity and formation of spherulites for linear PE. For high molecular weights and relatively low levels of crystallinity, spherulites are absent. For low molecular weights and high levels of crystallinity, well-developed spherulites are observed. The patterns in Figure 4 and the data of crystallinity in Table III are in good agreement with these conclusions. From the above analysis, patterns (c) and (g) seem to show a transitional region of supermolecular structure from the spherulites to the rodlike aggregates and randomly oriented lamellar structure. The data of gel content in Table III suggest that there is no indication of any spherulitic superstructure for gel contents above 60%, which is equivalent to the patterns obtained from more than 40 s irradiation below T_m (100°C) or more than 20 s irradiation above T_m (140°C). The patterns above 60% gel content could be representative of rodlike and disordered lamellar morphologies. Large changes in thermodynamic parameters such as density, melting point, and heat of fusion at gel contents above 60% in the previous work[1] were found concomitant with the more rapid changes of morphology. We can conclude that the overall effect of cross-linking on morphology is similar to that of an increase in the molecular weight of the polymer.[4,6,7]

Spherulitic Morphology of Photocross-linked LLDPE

Figure 5 shows the H_v patterns of LLDPE cross-linked below and above the melting point (126°C) with different irradiation times. The SALS patterns obtained below T_m are typical for a spherulitic morphology and do not differ significantly from those obtained above T_m. Spherulites observed tend to progressively deteriorate and become smaller as the irradiation time of cross-linking and the gel content increases, as shown in Table IV. The changes of the radii of spherulites in the samples cross-linked above T_m (140°C) are larger than those below T_m (100°C). However, all patterns display the four-leaf clover "tennis-racket" appearance for irradiation times increased to 80 s and cross-linked below or above T_m, apart from the fact that the light-scattering intensity is gradually stronger at the center and

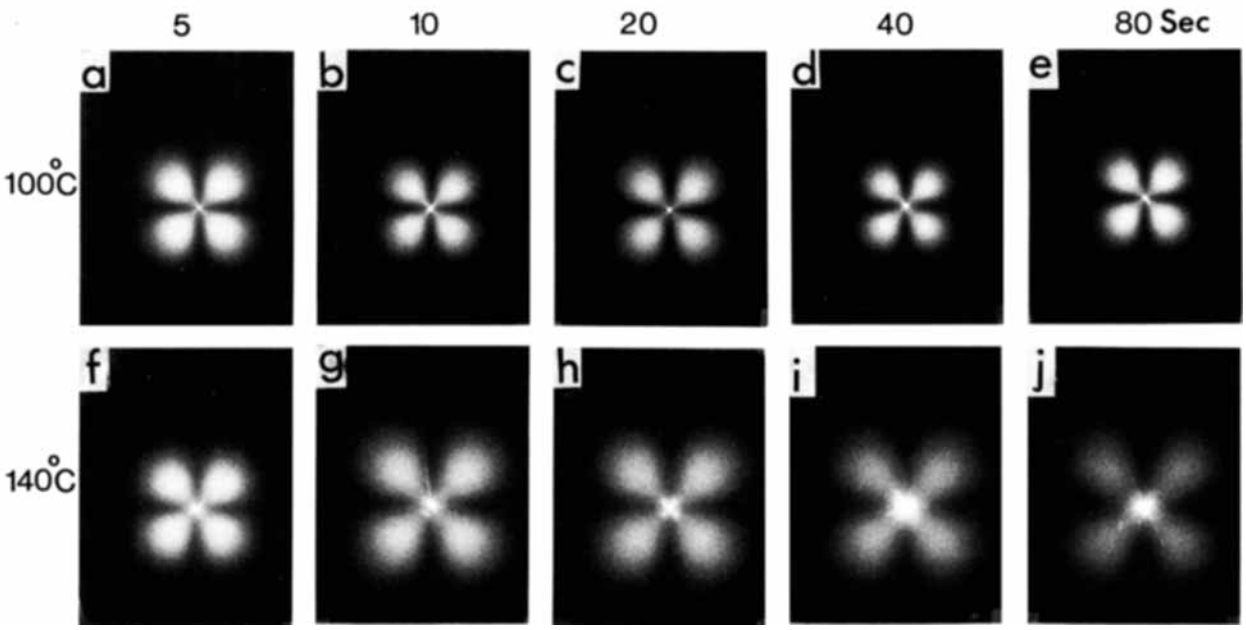

Figure 5 The effect of the degree of cross-linking on the spherulitic structures of LLDPE samples. Upper row: cross-linked at 100°C (below T_m)—(a) 5 s; (b) 10 s; (c) 20 s; (d) 40 s; (e) 80 s. Bottom row: cross-linked at 140°C (above T_m)—(f) 5 s; (g) 10 s; (h) 20 s; (i) 40 s; (j) 80 s.

the clover leaf weaker in the patterns obtained above T_m.

The fact that the highly cross-linked LLDPE sample [Fig. 5(j)] with 82% gel content (Table IV) still exhibits spherulitic morphology suggests that the morphological structures of cross-linked LLDPE could be affected not only by the degree of cross-linking but also by other structural units or microcrystals still present in the samples, at the cross-linking temperature of 140°C, that control the supermolecular morphology of LLDPE. It is well known that LLDPE molecules have linear sequences of PE interspersed by the relatively bulkier side chain of a comonomer (e.g., octene, butene, etc.). It has been reported[11] that the linear ethylene-rich regions and the branched portions in the LLDPE molecules have independent crystallization behavior. Wilfong and Knight[11] also found that even the most highly branched factions of LLDPE exhibited well-developed spherulites observed by SALS, which is similar to the above results shown in Figure 5 in this study. Therefore, that spherulitic morphologies of cross-linked LLDPE are relatively unaffected by the degree of cross-linking may be interpreted as due to the crystallization behavior correlated with the LLDPE molecular structure.

CONCLUSIONS

1. The supermolecular structure of photocross-linked polyethylene (XLPE) can be resolved by the small-angle light-scattering technique. Several different morphologies of XLPE have been deduced from H_v SALS patterns.

2. The supermolecular structure of XLPE is strongly dependent on the degree of cross-linking and the irradiation temperature during cross-linking. Increasing the degree of cross-linking causes a progressive deterioration of spherulitic morphology and development of other forms of superstructures such as rodlike aggregates and randomly oriented lamellae. The effect of photocross-linking is similar to that of increasing molecular weight on the morphological structure.[4,6,7] Cross-linking is a process by which polymer chains are chemically linked together to larger units. Therefore, the overall effect of cross-linking on morphology is similar to that of an increase in molecular weight of the polymer.

3. The SALS observations for photocross-linked PE samples suggest that the changes in supermolecular structure of XLPE correlate with the levels of degree of crystallinity. For highly cross-linked PE and relatively low levels of crystallinity, spherulitic

morphology is absent and, instead, rodlike or randomly orientated lamellae structure form. However, spherulitic morphology observed for LLDPE seems to correlate with the crystallization behavior of molecular structures of a copolymer.

This research work has been supported by a grant from The Swedish National Board for Technical Development (STU) and by a fellowship from the Wenner-Gren Foundation (to B.J.Q.), which is gratefully acknowledged. The authors also thank Dr. K. E. Russell, Kingston University, Ontario, Canada, for valuable discussions.

REFERENCES

1. B. J. Qu and B. Rånby, *J. Appl. Polym. Sci.*, to appear.
2. R. S. Stein and M. B. Rhodes, *J. Appl. Phys.*, **31,** 1873 (1960).
3. R. S. Stein, in *Structure and Properties of Polymer Film,* R. W. Lenz and R. S. Stein, Eds., Plenum Press, New York, 1973, p. 1.
4. S. Go, L. Mandelkern, R. Prud'homme, and R. S. Stein, *J. Polym. Sci. Polym. Phys. Ed.*, **12,** 1485 (1974).
5. T. Pakula, M. Kryszewski, and Z. Soukup, *Eur. Polym. J.*, **12,** 41, 47 (1976).
6. L. Mandelkern, S. Go, D. Peiffer, and R. S. Stein, *J. Polym. Sci. Polym. Phys. Ed.*, **15,** 1189 (1977).
7. J. Maxfield and L. Mandelkern, *Macromolecules,* **10,** 1141 (1977).
8. L. Mandelkern, *Discuss Faraday Soc.*, **68,** 310 (1979).
9. S. Bamji, A. Bulinski, J. Densley, and A. Garton, *IEEE Trans. Elect. Insulation,* **EI-18**(1), 32 (1983).
10. J. M. Rego Lopez and U. W. Gedde, *Polymer,* **30,** 22 (1989).
11. D. L. Wilfong and G. W. Knight, *J. Polym. Sci. Polym. Phys.*, **28,** 861 (1990).
12. M. B. Rhodes and R. S. Stein, *J. Appl. Phys.*, **32,** 2344 (1961); *J. Polym. Sci. Part A-2,* **7,** 1539 (1969).
13. R. S. Stein, P. F. Erhardt, S. B. Clough, and G. Adams, *J. Appl. Phys.*, **37,** 3980 (1966).
14. R. E. Prud'homme and R. S. Stein, *J. Polym. Sci. Polym. Phys. Ed.*, **12,** 1805 (1974).
15. Y. Akana and R. S. Stein, *J. Polym. Sci. Polym. Phys. Ed.*, **13,** 2195 (1975).
16. M. Moritani, N. Hayashi, A. Utsuo, and H. Kawai, *Polym. J.*, **2,** 74 (1971).
17. Y. Murakami, N. Hayashi, T. Hashimoto, and H. Kawai, *Polym. J.*, **4,** 452 (1973).
18. S. Nomura, M. Matsuo, and H. Kawai, *J. Polym. Sci. Polym. Phys. Ed.*, **12,** 1371 (1974).
19. T. Hashimoto, Y. Marakami, and H. Kawai, *J. Polym. Sci. Polym. Phys. Ed.*, **13,** 1613 (1975).
20. T. Hashimoto, K. Nagatoshi, A. Todo, and H. Kawai, *Polymer,* **17,** 1075 (1976).
21. D. G. Peiffer, *Polymer,* **32,** 134 (1991).
22. M. Motegi, T. Oda, M. Moritani, and H. Kawai, *Polym. J.*, **1,** 209 (1970).

Received October 15, 1992
Accepted December 3, 1992